Comparison between stability, electronic, and structural properties of cagelike and spherical nanodiamond clusters

M. Heidari Saani,[1,2] M. Kargarian,[3] and A. Ranjbar[3]
[1]*Semiconductor Component Industry, P.O. Box 19575-199, Tehran, Iran*
[2]*Physics Group, Maleke Ashtar University, P.O. Box 83145-115, Shahin Shahr, Iran*
[3]*Department of Physics, Sharif University of Technology, P.O. Box 11365-9161, Tehran, Iran*
(Received 8 August 2006; revised manuscript received 25 May 2007; published 17 July 2007)

Ab initio density functional theory calculations were used to investigate cohesive, electronic, and structural properties of cagelike and spherical hydrogen terminated nanoparticles of diamond. Unlike cagelike nanodiamond particles, the variation of calculated energies of spherical ones is not monotonic. The variation range of the calculated energies and bond lengths of cagelike nanoparticles is much tighter than the variation range of spherical ones. In contrast to spherical nanodiamond particles, the C-C bond lengths of all cagelike nanoclusters are very similar to the bond length of bulk diamond. The comparison of stability, electronic highest occupied molecular orbital-lowest unoccupied molecular orbital energy gaps, and structural properties of these two classes of nanodiamonds shows that the effects of spatial symmetry, morphology, and C-H atom ratio are more important than the effect of nanoparticle sizes.

DOI: 10.1103/PhysRevB.76.035417 PACS number(s): 73.22.−f, 81.07.−b

I. INTRODUCTION

Diamond nanoparticles have attracted much technological and theoretical interest in recent years.[1–5] They are hydrogen terminated nanoclusters of carbon atoms with sp^3 hybridization. The stability and optical properties of these particles are expected to be similar to unique properties of diamond[6–8] suggesting attractive applications in nanoscale device fabrication such as optoelectronics, electron emission devices, and nanoscale electromechanical systems. Other potential applications exist in pharmaceuticals and synthesizing byproducts of oil industry.[1] From theoretical point of view, quantum confinement effects in such systems are under investigations.[4] Other properties such as spin distribution in nitrogen-vacancy defect[9] and fullerenelike surface reconstructions[10] have been studied recently. High quality H terminated C nanoparticles can be isolated from petroleum.[1] Because of the difficulty in synthesizing different sizes of diamond nanoparticles and the early stages of experimental works on such systems,[5] theoretical investigations can be useful in analyzing physical properties of nanodiamond particles.[4]

In this paper, we investigate the effect of spatial symmetry, morphology, and different atomic configurations on cohesive, electronic, and structural properties of diamond nanoparticles. For this purpose, we study two different possible classes of the nanoparticles, including cagelike (diamondoids) and spherically symmetric hydrogen terminated nanoclusters. The cohesive and electronic properties of different sizes of nanoclusters are calculated and compared for both spherical and cagelike clusters. The observed difference between variations of physical properties of such clusters is attributed to the difference in the variations of C-H atom ratio and Mulliken atomic charge in the two classes of nanoclusters. The difference between dispersion of the value of calculated parameters of the two cluster types around the value of parameters of diamond lattice will be discussed.

II. CALCULATION METHOD

We employed *ab initio* density functional theory (DFT) cluster method[11] to calculate total energies and electronic structure of nanodiamond particles. The dangling bonds of the surfaces of diamond nanoparticles were saturated with H atoms. We performed a perfect geometry optimization of nanodiamond particles C_nH_m. In this optimization process, the root mean square of the Cartesian forces on each atom was reduced to 5 meV/Å. The cluster sizes that were used in our calculation with their related spatial symmetry and C-H atom ratio are summarized in Table I.

We used GAUSSIAN 03 code for self-consistent calculations of DFT.[12] The code gives single electron Kohn-Sham energy levels in real space representation for such clusters. The small atomic number of C atoms helped us do an all electron calculation. This calculation considers 1*s* core and 2*s*, 2*p* valence electrons and eliminates approximations that are required using different pseudopotentials. However, the contribution of the 1*s* core electrons in the calculated wave function of the highest filled energy levels is zero.

In this calculation, we used atomic centered 6-31G extended basis set for C and H atoms. Self-consistency of calculations was achieved when total energies converged by 10^{-5} a.u. We employed B3LYP hybrid exchange-correlation functional that includes the Becke[13] three parameter hybrid exchange functional. The formation energies per carbon atoms in different sizes of nanodiamond particles were calculated from the following formula:[2]

$$E_f(C_mH_n) = \frac{E(C_mH_n) - mE(C) - \frac{n-2}{2}E(H_2) - E(H_2)}{m}, \quad (1)$$

where $E(C_mH_n)$ is the calculated total energy. $E(C)$ and $E(H_2)$ are the calculated total energies of a single carbon atom and a H_2 molecule, respectively.

 ©2007 The American Physical Society

TABLE I. Different cagelike and spherical nanoparticles of diamond that were investigated in this calculation with the related spatial symmetries and C-H atom ratio.

Cagelike (spherical) nanoclusters	Symmetry	C-H atom ratio
$C_{10}H_{16}$ (C_5H_{12})	T_d (T_d)	0.625 (0.42)
$C_{14}H_{20}$ ($C_{17}H_{36}$)	C_{2h} (T_d)	0.7 (0.47)
$C_{18}H_{24}$ ($C_{29}H_{36}$)	C_{2v} (T_d)	0.75 (0.81)
$C_{22}H_{28}$ ($C_{35}H_{36}$)	C_{3v} (T_d)	0.79 (0.97)
$C_{22}H_{28}$ ($C_{47}H_{60}$)	C_1 (T_d)	0.79 (0.78)
$C_{22}H_{28}$	C_1	0.79
$C_{22}H_{28}$	C_{2h}	0.79
$C_{26}H_{32}$	C_1	0.81
$C_{26}H_{32}$	C_1	0.81
$C_{26}H_{32}$	T_d	0.81
$C_{30}H_{36}$	C_s	0.83
$C_{34}H_{38}$	C_1	0.89
$C_{38}H_{42}$	C_1	0.90
$C_{42}H_{46}$	C_1	0.91
$C_{45}H_{48}$	C_1	0.94

III. RESULTS AND DISCUSSION

In this section, we explain and discuss results concerning the variation of formation and electronic highest occupied molecular orbital-lowest unoccupied molecular orbital (HOMO-LUMO) energy gaps, C-H atom ratio, and Mulliken atomic charge versus nanoparticle size. We explain bond lengths and structural properties of cagelike and spherical nanodiamond particles. We also discuss the origin of the difference between variations of physical properties of the two types of nanoparticles. It should be noted that all of the calculated properties are obtained after a full relaxation of the structure of each nanoparticle. Final relaxed structures of spherical nanoparticles of Table I are shown in Fig. 1.

A. Formation energy properties

We show in Fig. 2 the results concerning formation energies of different sizes of cagelike and spherical nanodiamond particles.

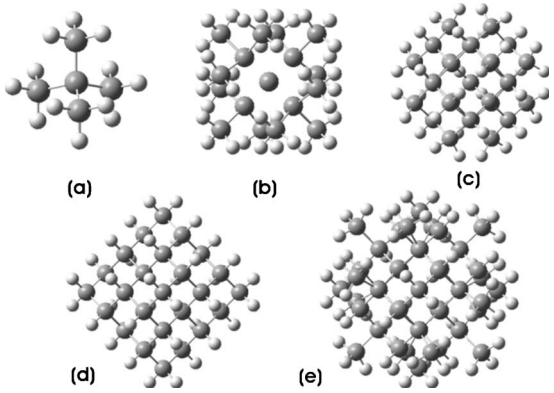

FIG. 1. Optimized atomic structure of spherical nanodiamond particles. (a) C_5H_{12}, (b) $C_{17}H_{36}$, (c) $C_{29}H_{36}$, (d) $C_{35}H_{36}$, and (e) $C_{47}H_{60}$.

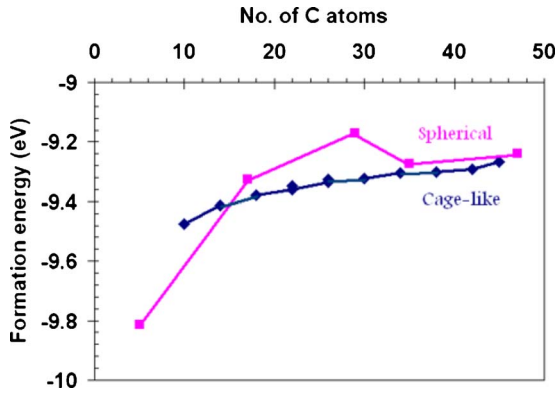

FIG. 2. (Color online) The variation of formation energy with the size of cagelike and spherical nanodiamond particles.

In this figure, in both classes of nanoclusters, by increasing the cluster sizes the formation energies increase. The formation energy increment is not linear and the rate of increment in larger cluster sizes decreases and tends to a constant value. The constant value is near the formation energy of diamond bulk. In Fig. 2, the increment in formation energies of the cagelike nanoclusters is monotonic. This is in agreement with reports of other groups on formation energies of nanodiamond particles.[2,3] This is also in agreement with reported results concerning formation energy variation with the radius of spherical Si and Ge nanoparticles.[14] Unlikely, in Fig. 2 for the spherical nanodiamond particles, the formation energy reaches a maximum value for the $C_{29}H_{36}$ nanocluster. In this figure, for clusters larger than $C_{29}H_{36}$, the value of the formation energy decreases. In Fig. 2, one can realize that in contrast to cagelike nanodiamond particles, the most stable spherical nanoparticle is not the largest one and it is the $C_{29}H_{36}$.

We have also calculated variation of formation energy versus radius of the different sizes of spherical nanoclusters and similar nonmonotonic variations were reproduced. The formation energy of the cagelike nanodiamond particles increases continually from −9.47 eV for the $C_{10}H_{16}$ cluster to −9.27 eV for the $C_{45}H_{48}$ cluster, while the formation energy of the spherical nanodiamond particles increases from −9.81 eV for the C_5H_{12} cluster to −9.24 eV for the $C_{47}H_{60}$ cluster where there is a maximum value in $C_{29}H_{36}$ cluster. Hence, the range of variation of formation energy with the size for spherical nanodiamond particles is about 0.57 eV, which is much larger than that of cagelike nanodiamond particles which is 0.20 eV. In other words, the values of formation energy of the cagelike nanodiamond particles are much closer to each other than the formation energies of spherical nanodiamond particles. This is in agreement with experimentally investigated abundance of different sizes of cagelike nanoclusters.[1] Based on the formation energy calculations, the larger sizes of spherical nanoparticles could have similar abundance as cagelike ones, while for smaller spherical nanodiamonds only $C_{29}H_{36}$ is much more stable than cagelike nanoclusters with similar sizes.

In order to distinguish the probable effect of the difference in the number of the C atoms and the effect of morphology on the relative formation energies of the cagelike and

TABLE II. The formation energies of such cagelike and spherical nanodiamond particles which have almost the same number of C atoms with the corresponding spatial symmetries and C-H atom ratios.

Cagelike (spherical) clusters	Symmetry	Formation energy (eV)
$C_{18}H_{24}$ ($C_{17}H_{36}$)	C_{2v} (T_d)	−9.38 (−9.33)
$C_{30}H_{36}$ ($C_{29}H_{36}$)	C_s (T_d)	−9.32 (−9.17)
$C_{34}H_{38}$ ($C_{35}H_{36}$)	C_1 (T_d)	−9.30 (−9.27)

spherical clusters, we compare such clusters from these two classes of nanodiamond particles which have almost the same number of the C atoms. Results are summarized in Table II.

The formation energies listed in this table indicate that the clusters with almost the same number of C atoms (the same size) have not the same formation energies. The difference between formation energies of cagelike and spherical nanodiamond particles varies from 0.03 eV for the $C_{34}H_{38}$ and $C_{35}H_{36}$ clusters up to 0.15 eV for the $C_{30}H_{36}$ and $C_{29}H_{36}$ nanoclusters. In Table II, although the comparing clusters from two classes have almost the same number of the C atoms, the spherical nanoclusters have larger formation energies than the cagelike ones. This comparison shows that the effect of spatial symmetry and morphology is more important than the size effect on the formation energy of nanoparticles. However, for the largest sizes of nanodiamonds that are listed in Table II, the difference between the formation energies of the two classes is very small and is comparable to the thermal activation energy at room temperature (25 meV).

B. Electronic properties

The HOMO-LUMO energy gaps of nanodiamond particles were calculated from the energies of the highest occupied and the lowest unoccupied Kohn-Sham molecular orbitals for cagelike and spherical nanoparticles. The results are shown in Fig. 3. Similar to previously reported results,[2–4] we observe a monotonic reduction of electronic HOMO-LUMO energy gaps with the cluster size for cagelike nanoparticles. The HOMO-LUMO energy gaps of the cagelike nanodiamond particles decrease continually from 9.3 eV for the $C_{10}H_{16}$ cluster to 7.7 eV for the $C_{45}H_{48}$ nanocluster. For spherical nanoparticles, our calculation indicates that the HOMO-LUMO energy gaps of the spherical nanodiamond particles decrease from 10.6 eV for the C_5H_{12} cluster to 7.9 eV for the $C_{47}H_{60}$ cluster. This reduction is not monotonic and the value of HOMO-LUMO energy gaps reaches a minimum value in $C_{35}H_{36}$ cluster. The difference between HOMO-LUMO energy gaps of the two largest clusters $C_{35}H_{36}$ and $C_{47}H_{60}$ is 0.1 eV.

The variation ranges of HOMO-LUMO energy gaps are 1.6 and 2.8 eV for the cagelike and spherical nanoparticles, respectively. Similar to variation range of formation energies, the dispersion of HOMO-LUMO energy gap values for the cagelike nanodiamond particles is much smaller than the

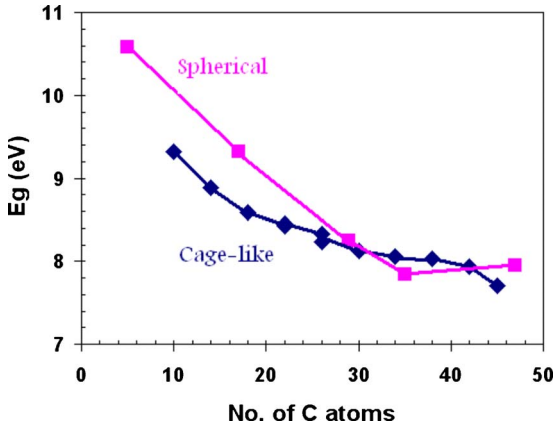

FIG. 3. (Color online) The variation of electronic HOMO-LUMO energy gaps with the size of cagelike and spherical nanodiamond particles.

dispersion of HOMO-LUMO energy gap values of the spherical ones. For smaller sizes of nanoparticles, the HOMO-LUMO energy gaps of spherical nanoparticles are much larger than those of the cagelike ones; however, by increasing the size up to $C_{29}H_{36}$ cluster, the HOMO-LUMO energy gap of cagelike nanoclusters exceeds the HOMO-LUMO energy gap of the spherical ones (Table III). In summary, the variation of HOMO-LUMO energy gaps for the cagelike nanoparticles versus size is more monotonic and much slower than that for the spherical ones.

For larger sizes of the nanoclusters, the HOMO-LUMO energy gaps of both classes of clusters converge to a common energy value that is about 8.0 eV. This reduction of HOMO-LUMO energy gaps or reduction of quantum confinement effect may represent transformation from a molecular to a bulk system. A similar trend has been reported for variation of HOMO-LUMO energy gaps with the size for Si and Ge nanoparticles.[15–17]

In Table III, we have listed such nanoclusters from cagelike and spherical types that have almost the same number of C atoms (similar sizes) in order to compare HOMO-LUMO energy gaps independent of the nanoparticle sizes. The HOMO-LUMO energy gaps listed in this table indicate that the nanoclusters with almost the same number of C atoms have not the same electronic HOMO-LUMO energy gaps. The difference between HOMO-LUMO energy gaps of cagelike and spherical nanodiamond particles varies from 0.13 eV for the $C_{30}H_{36}$ and $C_{29}H_{36}$ up to 0.7 eV for the $C_{17}H_{36}$ and $C_{18}H_{24}$ nanoclusters. This comparison shows that

TABLE III. In this table, we have listed the electronic HOMO-LUMO energy gap of such cagelike and spherical nanodiamond particles, which have almost the same number of C atoms.

Cagelike (spherical) clusters	Symmetry	HOMO-LUMO gap energy (eV)
$C_{18}H_{24}$ ($C_{17}H_{36}$)	C_{2v} (T_d)	8.59 (9.32)
$C_{30}H_{36}$ ($C_{29}H_{36}$)	C_s (T_d)	8.12 (8.25)
$C_{34}H_{38}$ ($C_{35}H_{36}$)	C_1 (T_d)	8.06 (7.84)

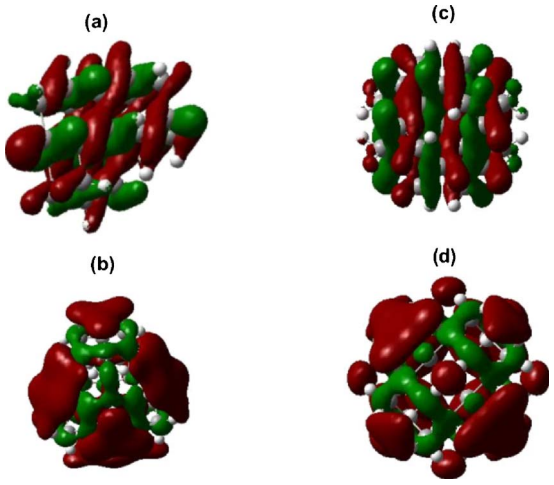

FIG. 4. (Color online) The isocharge surface of (a) HOMO and (b) LUMO states of cagelike nanodiamond particles. The isocharge surface of (c) HOMO and (d) LUMO states of spherical nanodiamond particles.

the effects of the spatial symmetry and morphology on the HOMO-LUMO energy gaps similar to formation energy are more important than the effect of size of the nanoparticles.

We show in Fig. 4 the shape of isocharge surface of single electron HOMO and LUMO states for cagelike and spherical nanodiamond particles. In this figure, one can realize that for both classes of nanodiamond particles in the HOMO states, there is a considerable probability of finding electrons inside a nanoparticle and especially in bonds between C atoms. However, for LUMO states there is a considerable probability of finding electrons outside the nanoparticles and the surface H atoms are almost screened by LUMO electrons. This delocalization of electrons in LUMO state of nanodiamond particles has been used to explain the absence of quantum confinement effect for the energy of LUMO.[4] In this figure, we find that there is not any notable difference between isocharge surface of HOMO and LUMO states of cagelike and spherical nanodiamond particles.

C. Effect of C-H atom ratio and Mulliken atomic charge on calculated energies

As the size of the nanoparticles increases, the number of C atoms in comparison with the number of H atoms or the carbon-hydrogen atom ratio increases. The trends of variation of C-H atom ratio for cagelike and spherical nanoparticles are shown in Fig. 5.

Considering reduction of H atoms in comparison to bulk C atoms by increasing the cluster size, we expect that the induced net charge in the bulk of nanoclusters due to the difference in electronegativity of the C and H atoms decreases. Our results show that there is a gradient of net charge from the H atoms on the surface toward the C atoms at the center of each cluster. The gradient of charge alters the perfect covalent character of C-C bonds to a partially polar one. Consequently, the C-C bonds in such hydrocarbon nanoclusters are not as stable as the perfectly covalent C-C bonds in a diamond lattice. In other words, by decreasing the relative number of H atoms with respect to C atoms (increasing the C-H atom ratio), the gradient of net charge decreases, resulting to a much stable nanodiamond particle. To justify this interpretation, we calculated formation energies of C atoms in CH_4 and C_2H_6 molecules. The corresponding formation energy values per C atom for these molecules are −0.32 eV (for CH_4) and −0.30 eV (for C_2H_6). The values of C-H atom ratio for these molecules are 0.25 and 0.33, respectively. Also, the net induced charges on the C atoms are also −0.58 and −0.40 for CH_4 and C_2H_6, respectively. In the methane molecule where the C atom bonds to four H neighboring atoms (four partially polar bond), the induced charge is more than that in the ethane molecule which has three partially polar C-H and a more covalent C-C bond. In this instance, by increasing the C-H atom ratio the formation energy of C_2H_6 increases and the induced charge on the related C atom decreases with respect to CH_4. Moreover, the HOMO-LUMO energy gaps of methane and ethane molecules are 14.1 and 12.1 eV, respectively, which are consistent with the decrement of HOMO-LUMO energy gap with increasing C-H atom ratio.

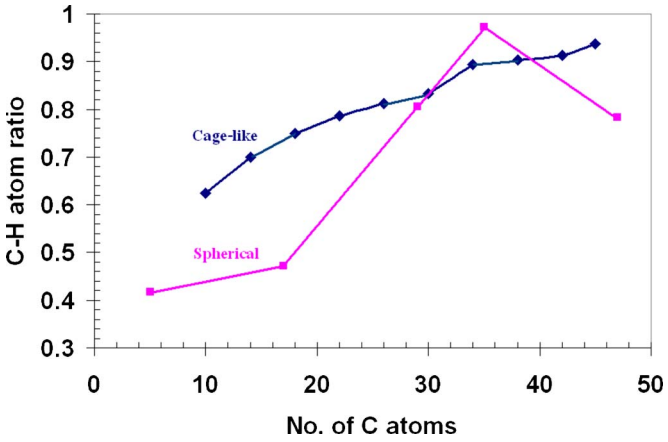

FIG. 5. (Color online) The variation of C-H atom ratio with the size of cagelike and spherical nanodiamond particles.

We also calculated Mulliken induced charge for different sizes of cagelike and spherical nanodiamond particles. The results of spherical ones are shown in Fig. 6. Similar to Ref. 3, we observe a significant reduction in the induced atomic

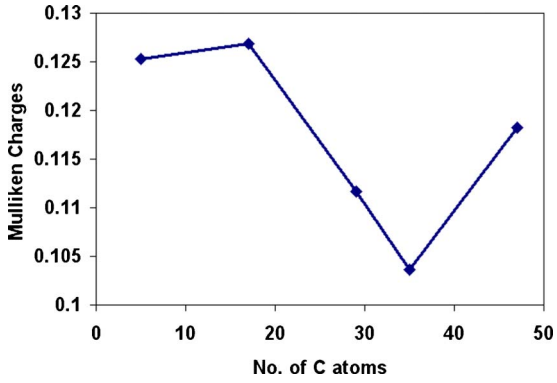

FIG. 6. (Color online) The variation of Mulliken atomic charge with the size of spherical nanodiamond particles.

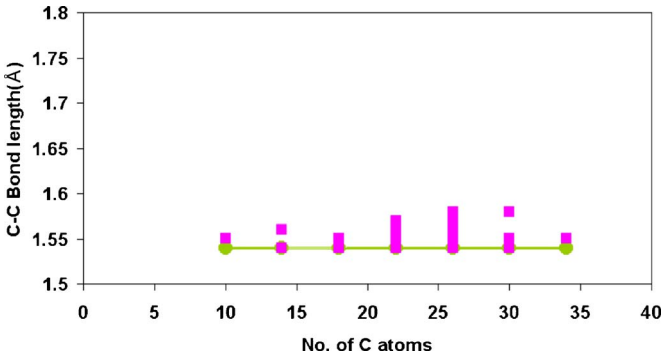

FIG. 7. (Color online) The calculated C-C bond lengths of cagelike nanodiamond particles with different sizes. The solid line shows the C-C bond lengths of diamond lattice.

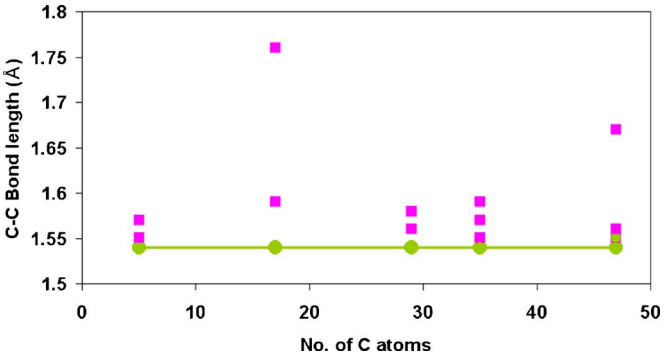

FIG. 8. (Color online) The calculated C-C bond lengths of each spherical nanodiamond particle with different sizes. The solid line shows the C-C bond lengths of diamond lattice.

net charge on C atoms of spherical nanoparticles by increasing the cluster size. This reduction of charge is due to the increase in the number of the C-C bonds with respect to the number of partially polar C-H bonds. In Fig. 6, for spherical nanodiamond clusters, the variation of induced charge is not monotonic. The monotonic variation for cagelike nanocluster has been reported previously in Ref. 3. There is a minimum value for induced net charge at $C_{35}H_{36}$ cluster in Fig. 6. The minimum atomic Mulliken charge of spherical $C_{35}H_{36}$ cluster is in very good agreement with the results concerning C-H atom ratio in Fig. 5. In this figure, the C-H atom ratio has a maximum value for the $C_{35}H_{36}$ nanocluster. Therefore, the variations of C-H atom ratio and Mulliken atomic charge in the spherical nanoparticles are not monotonic and have maximum and minimum values, respectively. This behavior is coherent with the variation of the formation and electronic HOMO-LUMO energy gaps that have minimum values for spherical clusters. For cagelike nanodiamond particles, the variation of the C-H atom ratio is monotonic, in agreement with the monotonic variation of the formation energy and electronic HOMO-LUMO energy gaps.

By comparing the results of variations of formation energies, HOMO-LUMO energy gaps, and C-H atom ratio versus size in Figs. 2, 3, and 5 and also the variation of Mulliken atomic charge versus size in Fig. 6, we could conclude that there is a correlation between variations of Mulliken atomic charge and C-H atom ratio with the formation energy and HOMO-LUMO energy gaps.

D. Structural properties

From the geometry optimization of cagelike and spherical nanoclusters, we obtained the equilibrium C-C bond lengths for different sizes of nanoparticles. The variation of the C-C bond lengths versus the size of cagelike and spherical nanoparticles is shown in Figs. 7 and 8, respectively.

As it has been shown in Fig. 7, the C-C bond lengths in cagelike nanoparticles are very close to the equilibrium bond lengths of the C-C bond lengths in a diamond lattice, i.e., 1.54 Å. In this class of nanoclusters, the bond lengths vary from 1.54 up to 1.58 Å. It is interesting to note that the lower limit of our obtained bond lengths for cagelike clusters is 1.54 Å; in other words, all of the relaxed bond lengths are larger than the equilibrium bond lengths of a diamond lattice.

In contrast to cagelike nanodiamond particles, in Fig. 8 the values of C-C bond lengths of spherical nanodiamond particles are much more dispersive. The range of variation of the bond lengths in spherical clusters is from 1.54 up to 1.76 Å. Similar to cagelike nanodiamond particles, all of the C-C bond lengths in spherical clusters are larger than 1.54 Å, which is the equilibrium bond length of diamond.

In Fig. 1, we showed the optimized atomic structure of spherical nanoclusters. The spherical nanoparticles that have bond lengths close to the bond lengths of diamond lattice and the ones which have bond lengths much larger than 1.54 Å can be distinguished in this figure. In Fig. 1, the C-C bond lengths of C_5H_{12}, $C_{35}H_{36}$, and $C_{29}H_{36}$ nanoparticles are very close to the C-C bond lengths of a diamond lattice (1.54 Å). In contrast, the C-C bond lengths of $C_{17}H_{36}$ and $C_{47}H_{60}$ nanoparticles have a large deviation from the corresponding value of a diamond lattice.

For each nanocluster, there are different values for C-C bonds depending on the different locations of the C-C bond with respect to the center of the nanocluster. We show in Fig. 9 the variation of C-C bond length versus distance from the center of $C_{47}H_{60}$ spherical nanoparticle. Overall, the C-C bond lengths in the central part of nanodiamond particles are larger than those near the surface. As reported in the literature,[14] both Si and Ge nanocrystals passivated with hydrogen exhibit an expansion of the Si-Si or Ge-Ge bond

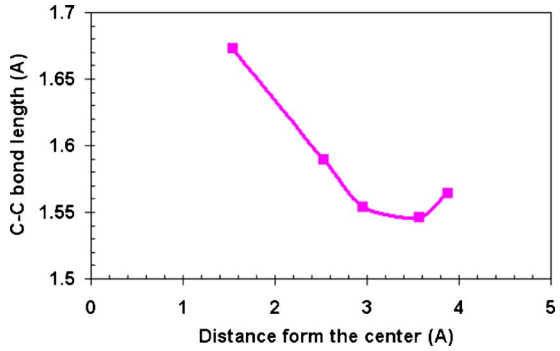

FIG. 9. (Color online) The calculated C-C bond lengths of $C_{47}H_{60}$ spherical nanodiamond particle versus distance from the center of the nanoparticle.

lengths with respect to their bulk value at the center of the nanocrystals and a contraction of the same bonds near the surface, in agreement with our results for diamond nanoparticles in Fig. 9.

IV. CONCLUSION

Using *ab initio* DFT calculations, we studied cohesive, electronic, and structural properties of different morphologies and sizes of nanodiamond particles. Our results show that the variations of the formation energy and HOMO-LUMO energy gaps with the size are different for the two classes of nanodiamond particles. These variations correlate strongly with the variations of the C-H atom ratio and Mulliken atomic charge for both classes of nanoparticles. This suggests that the morphology, spatial symmetry, and C-H atom ratio govern physical property of the nanoclusters. Unlike spherical nanodiamond particles, the structure and bond lengths of all cagelike nanodiamond particles are very close to the structure of bulk diamond. The dispersion of calculated physical properties especially the formation energies of the cagelike clusters is much smaller than the dispersion of the parameters of the spherical ones. This may explain the coexistence of different sizes of cagelike nanodiamond particles. Finally, we found that the formation energy of the large spherical nanoparticles is comparable with that of the cagelike ones. The latter have been observed experimentally.

[1] J. E. Dahl, S. G. Liu, and R. M. K. Carlson, Science **299**, 96 (2003).
[2] G. C. McIntosh, M. Yoon, S. Berber, and D. Tomanek, Phys. Rev. B **70**, 045401 (2004).
[3] A. J. Lu, B. C. Pan, and J. G. Han, Phys. Rev. B **72**, 035447 (2005).
[4] N. D. Drummond, A. J. Williamson, R. J. Needs, and G. Galli, Phys. Rev. Lett. **95**, 096801 (2005).
[5] T. M. Willey, C. Bostedt, T. van Buuren, J. E. Dahl, S. G. Liu, R. M. K. Carlson, L. J. Terminello, and T. Moller, Phys. Rev. Lett. **95**, 113401 (2005).
[6] R. P. Messmer and G. D. Watkins, Phys. Rev. B **7**, 2568 (1973).
[7] J. P. Goss, R. Jones, S. J. Breuer, P. R. Briddon, and S. Oberg, Phys. Rev. Lett. **77**, 3041 (1996).
[8] M. H. Saani, M. A. Vesaghi, K. Esfarjani, T. G. Elahi, M. Saiari, A. Hashemi, and N. Gorjizadeh, Phys. Rev. B **71**, 035202 (2005).
[9] V. A. Pushkarchuk, S. Ya. Kilin, A. P. Nizovtsev, A. L. Pushkarchuk, V. E. Borisenko, C. von Borczyskowski, and A. B. Filonov, Opt. Spectrosc. **99**, 245 (2005).
[10] J.-Y. Raty, G. Galli, C. Bostedt, T. W. van Buuren, and L. J. Terminello, Phys. Rev. Lett. **90**, 037401 (2003).
[11] R. Jones and P. R. Briddon, in *Identification of Defects in Semiconductors*, edited by M. Stovela, Semiconductors and Semimetals Vol. 51A (Academic, Boston, 1998), Chap. 6.
[12] M. J. Frisch, G. W. Trucks, H. B. Schlegel, G. E. Scuseria, M. A. Robb, J. R. Cheeseman, V. G. Zakrzewski, J. A. Montgomery Jr., R. E. Stratmann, J. C. Burant, S. Dapprich, J. M. Millam, A. D. Daniels, K. N. Kudin, M. C. Strain, O. Farkas, J. Tomasi, V. Barone, M. Cossi, R. Cammi, B. Mennucci, C. Pomelli, C. Adamo, S. Clifford, J. Ochterski, G. A. Petersson, P. Y. Ayala, Q. Cui, K. Morokuma, D. K. Malick, A. D. Rabuck, K. Raghavachari, J. B. Foresman, J. Cioslowski, J. V. Ortiz, A. G. Baboul, B. B. Stefanov, G. Liu, A. Liashenko, P. Piskorz, I. Komaromi, R. Gomperts, R. L. Martin, D. J. Fox, T. Keith, M. A. Al-Laham, C. Y. Peng, A. Nanayakkara, C. Gonzalez, M. Challacombe, P. M. W. Gill, B. Johnson, W. Chen, M. W. Wong, J. L. Andres, C. Gonzalez, M. Head-Gordon, E. S. Replogle, and J. A. Pople, GAUSSIAN 03, Revision B.04, Gaussian, Inc., Pittsburgh PA, 2003.
[13] A. D. Becke, J. Chem. Phys. **98**, 5648 (1993).
[14] L. E. Ramos, J. Furthmüller, and F. Bechstedt, Phys. Rev. B **72**, 045351 (2005).
[15] S. Öğüt, J. R. Chelikowsky, and S. G. Louie, Phys. Rev. Lett. **79**, 1770 (1997).
[16] E. Degoli, G. Cantele, E. Luppi, R. Magri, D. Ninno, O. Bisi, and S. Ossicini, Phys. Rev. B **69**, 155411 (2004).
[17] Y. Maeda, Phys. Rev. B **51**, 1658 (1995).